Arab J. Nucl. Sci. Appl., Vol. 57, 3, 24-34 (2024)

ISSN 1110-0451

Arab Journal of Nuclear Sciences and Applications

Web site: ajnsa.journals.ekb.eg

(E S N S A)

Proposed New Different Coincidence Neutron Detection Systems using Monte Carlo Simulation

R.A. El-Tayebany[1] and Mootaz Ebied SHALAF[2]

[1] *Nuclear and Radiological Safety Research Center, Egyptian Atomic Energy Authority, Cairo, Egypt*
[2] *National Center for Radiation Research and Technology, Egyptian Atomic Energy Authority, Cairo, Egypt*

ARTICLE INFO

Article history:

Received: 3rd May 2024
Accepted: 24th June 2024
Available online: 5th July 2024

Keywords:

MCNPX,
Active Well (AWCC),
^{3}He, Ar, BF_3, AmLi,
AmBe and ^{252}Cf.

ABSTRACT

In this work, new designs for coincidence neutron detection systems were proposed and assessed with different neutron detectors (^{3}He, Ar and BF_3) and calculations. Each system consists of 42- neutron detectors arranged in two rings. The simulated systems include special nuclear material (SNM) with changing the neutron sources such as; AmLi, AmBe and ^{252}Cf. The aim of this work is the determination of the coincidence system efficiency and neutron distribution fluence for each proposed system in active mode with a changing of neutron detectors arrangement. The results of the proposed systems were studied and compared to the active-well neutron coincidence counter (AWCC) which is employed in uranium testing using the code Monte Carlo N-Particle eXtended (MCNPX) version 2.7.0. The systems that were suggested fell within the energy range of 0-0.025 KeV, which is the thermal neutron region. The results proved that we could advocate implementing any of the presented ideas to replace AWCC because no single model outperformed the others.

1. INTRODUCTION

Neutron multiplicity and coincidence detectors are commonly employed in measuring and verifying nuclear material for safeguards purposes. Monte Carlo codes could be used to simulate detectors in order to aid in calibration, design, optimization, and analysis of the detection system. On the other hand, it could be used to predict the behavior of particles and radiation within detectors or proposed new systems [1-3].

Simulation must take into account factors such as neutron source spectrum, direction, fission neutron multiplicity, and the detection of thermalized neutrons by proposed counters. In many cases where for example regular measurements are either unavailable or there are no representative reference materials, Monte Carlo simulation codes may be the best possible solution [4,5].

the AWCC contains two AmLi neutron sources in its active mode in addition to 3He detectors. Neutron coincidence detectors use AmLi neutron sources because a single neutron is released by a single (alpha,n) process.. However, AmLi sources are not easily available nowadays, and the search for alternative neutron sources became a necessity.

Using AWCC, the AmBe source was examined; the findings indicated that compared to the AmLi source, the AmBe source has a background with a greater number of singles and doubles. Conversely, AmBe's net induced fission singles and doubles rate was lower than AmLi's. This demonstrates that AmBe can be used in the AWCC instrument in place of AmLi [6]. AmLi and ^{10}B, two interrogation sources used in AWCC, were studied to obtain their optimal neutron energy spectrum. Using Monte Carlo simulations, it was determined the spectra of AmLi and ^{10}B sources as well as the neutron spectrum as measured beyond the encapsulation of a source. Numerous factors influencing energy distributions and photon and neutron emissions have been examined [7]. The production of several neutrons per spontaneous fission by the interrogation source, which is time dependent with the sample's induced fissions (IF), is a special advantage of ^{252}Cf sources. Consequently, the

Corresponding author: rreltyebany@gmail.com
DOI: 10.21608/AJNSA.2024.287054.1814

doubles signal increases and statistical error lowers. Certain studies have chosen to use ^{252}Cf in place of AmLi as the interrogation source for the Uranium Neutron Coincidence Collar (UNCL), as well as, the Active Well Coincidence Counter (AWCC) [8,9].

2. DETECTORS AND INTERROGATION SOURCES

^{3}He Gas filled Detectors

Although there is a recent shortage in its global supply, The most effective neutron detectors are 3He-filled proportional counters due to the fact that they have a high cross-section of neutrons are less sensitive to gamma rays, are not corrosive or toxic, able to endure difficult circumstances as well as having the ability to run at a lower voltage than certain other proportional counter options. There isn't enough 3He left in the globe to meet demand because its supply is extremely limited. Thus, research is being done on substitute neutron detectors. Because compared to 3He, boron trifluoride detectors are less sensitive., they are not suitable in all circumstances. It requires a voltage far higher than that of 3He detectors and is corrosive. A. Lintereur et al. (2011) measured the relationship between tube pressure and the 3He and boron trifluoride neutron detection effectiveness. Models of the radiation portal monitor systems were also validated using the experimental results [10].

BF_3 proportional counter

As BF_3 is much more available than ^{3}He, so common neutron detector is the BF3 filled proportional counter. A slow neutron can form A α-particle that can have two different energies (2.31 and 2.79 MeV) when it interacts with boron-10. Due to its short range, the α-particle generated in this way interacts with gas molecules fast, leading to the creation of pairs of electrons and ions. The avalanche is started by the electrons when exposed to a powerful electric field. This technique of gas multiplication guarantees a large pulse at the readout electrode and is characteristic of proportional counters. Because of the neutrons' excellent energy deposition, BF_3 counters have excellent neutron-discriminating capabilities [11].

Ar Gas filled Detectors

Excellent behavior for counting the fission products is shown by a recent study on the argon gas detector. A fission detector designed for the First Energy Amplifier Test at the CERN-PS was described by F. Casagrandei et al. The system is a compact, high-pressure Argon gas ionization chamber that exhibits exceptional efficiency for Fission Fragments and strong background rejection. Both the detector's placement and its impact on the neutron flux distribution have an impact on the total neutron efficiency as determined by the experiment [12]. Additionally, Radiation detection has generally made use of Ar/CO_2, a detector counting gas. These days, one of the expanding uses for Ar/CO_2-filled detectors is neutron detection [13].

Interrogation sources

The choice of interrogation source as ^{252}Cf, AmLi and AmBe to be used with Coincidence Neutron Detection Systems, is very important. Since there is always one neutron released by a single (alpha, n) reaction. with multiplicity, AmLi and AmBe sources could be employed. Neutron emission overlap is accidental and easily explained. The production of neutrons occurs independently of each other and is unrelated to energy, direction, and multiplicity. On the other hand, numerous neutrons are released during a single ^{252}Cf spontaneous fission event, which has the potential to cause time-dependent fissions with the remaining neutrons [14].

3. COINCIDENCE NEUTRON SYSTEMS SIMULATION

MCNP simulation

This input file sets up a basic simulation scenario in MCNP. Depending on the complexity of the problem, input files can be significantly more detailed and include additional cards and specifications. The first line of the input file is a comment line that usually contains the problem title or a brief description of the simulation. This line is for documentation purposes and is ignored by the MCNP code. Cell Cards define the geometry and materials of the problem. Each cell card specifies a region of space (cell), the material it contains, and its density. The cell Number is a unique identifier for the cell. The material Number Corresponds to the material defined in the material cards. the material density is specified in atoms/barn-cm or in g/cm³ (negative for mass density). The surface Specification defines the boundaries of the cell using surface numbers. Importance for neutrons and photons (used in variance reduction). Surface Cards define the surfaces that bound the cells. Each surface card specifies a surface using geometric parameters. Surface Number is a unique identifier for the surface. Surface type Indicates the type of surface (e.g., plane, cylinder, sphere), as well as, coordinates and other parameters defining the surface. Data cards Provide

additional information required for the simulation, such as material compositions, source definitions, tally specifications, and physics options. Material cards define the materials used in the cells. The material number Corresponds to the material number in the cell cards. Isotope composition specifies the isotopes and their fractions. Source definition cards describe the characteristics of the neutron or photon source. The source distribution Specifies the spatial, energy, and angular distribution of the source particles. The tally cards define the quantities to be measured (e.g., flux, dose). The tally number is an identifier for the tally and determines the type of measurement (e.g., F4 for flux, F6 for energy deposition). Also, the energy bin is a defined range of energies used to tally or categorize the energy distribution of particles, such as neutrons or photons, as they interact with materials in the simulation. Energy bins are crucial for analyzing the energy spectrum of particles, understanding their behavior, and evaluating the results of the simulation. [15-17].

The neutron reaction rate in the detector (such as the ^{3}He(n,p) rate in a ^{3}He detector) can be used to estimate the pulse-counting rate of the detector with adequate accuracy in many applications. This is a good approximation for ^{3}He and BF_3 tubes in typical usage scenarios. For detectors like boron-lined proportional counters, where a portion of the reaction product energy is deposited in the boron layer instead of the gas, a more comprehensive method is required. Additional examples are organic scintillators and 4He detectors, where the signal is generated by the recoil of 4He or H nuclei formed by neutron elastic scattering. we can notice that 3He(n,p) reactions and 3He elastic scattering both affect the measured rates in 3He spectrometers. A more thorough treatment is required because, in each of these scenarios, a neutron reaction does not always result in a pulse above the threshold in the detector. These scenarios can be calculated using MCNPX. The following actions must be included in the input file: create the reaction products and/or elastic recoils, track these charged particles in the actual detector gas, and tally the energy deposited in the active volume of the detector [18].

A coincidence neutron counting system is the active-well neutron coincidence counter (AWCC). It was created to test ^{235}U-bearing materials in a non-destructive technique. The AWCC operates by employing interrogation neutron emitters to find coincidence neutrons produced by the ^{235}U isotope's induced fission. Its primary parts are two rings of neutron detectors encircling an assaying chamber that are inserted in a polyethylene moderator. End plugs with caps and bottoms shield the interrogation sources from neutrons while also acting as reflectors to lower neutron end losses and improve counting efficiency. The inside of the polyethylene moderator has an Al–Cd This detector well cover enhances the protection between the detectors and the neutron sources through preventing thermal neutrons from reaching the interrogation flow. In the existence of cadmium cover, the AWCC is thought to be operating in rapid mode. Large volumes of ^{235}U can be assayed with the counter due to the neutron spectrum's relatively high energy. The AWCC operates in the thermal mode when the Al–Cd sleeve is removed. Because of the counter's much-increased sensitivity and comparatively low energy neutron spectrum, it is appropriate for determining low enriched uranium samples [19,20]. In this work, we simulated eight systems of neutron detectors that take the same design as AWCC with different neutron detector types and arrangements using MCNPX (version 2.7.0). These systems are shown in fig.(1). It consists of the simulated AWCC design as in model (a) where the inner and outer rings are composed of the same type of neutron detector which is ^{3}He neutron detector while the model (b) contains inner ring from Ar detector while the outer ring is from ^{3}He detectors and vice versa in the model (d). In model (c), the inner ring from BF_3 detectors and the outer ring from ^{3}He detectors and vice versa in model (e). In model (f), both rings are from Ar detectors, and in model (g) both rings are from BF_3 detectors

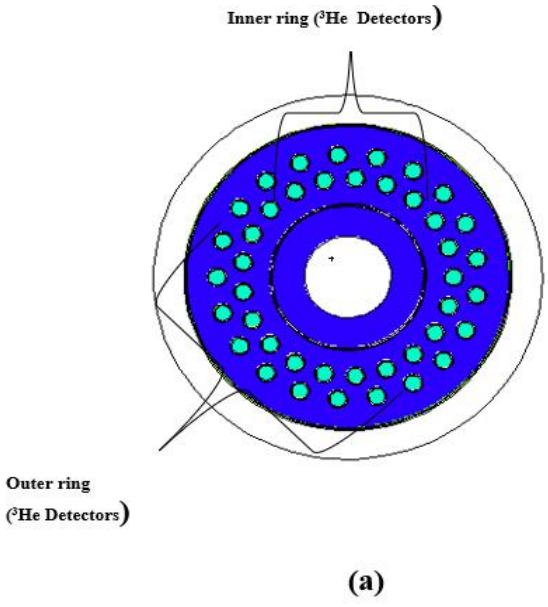

(a)

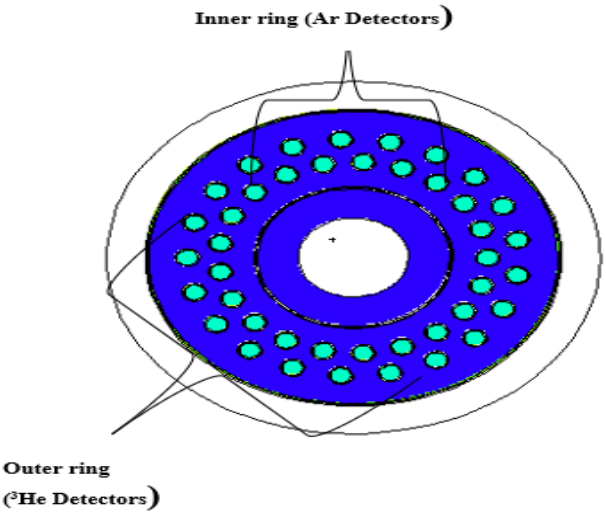
Inner ring (Ar Detectors)
Outer ring
(³He Detectors)

(b)

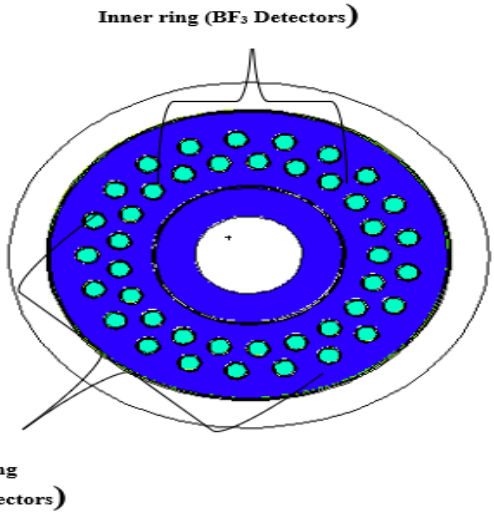
Inner ring (BF₃ Detectors)
Outer ring
(³He Detectors)

(c)

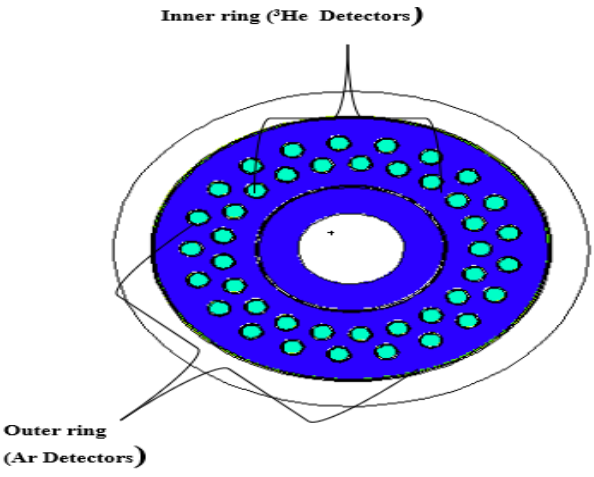
Inner ring (³He Detectors)
Outer ring
(Ar Detectors)

(d)

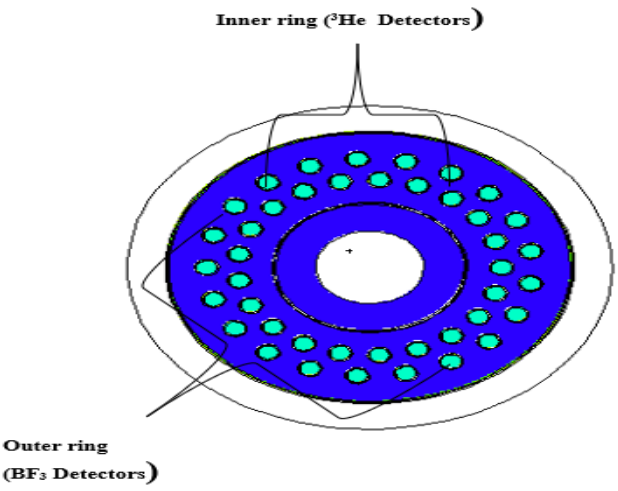
Inner ring (³He Detectors)
Outer ring
(BF₃ Detectors)

(e)

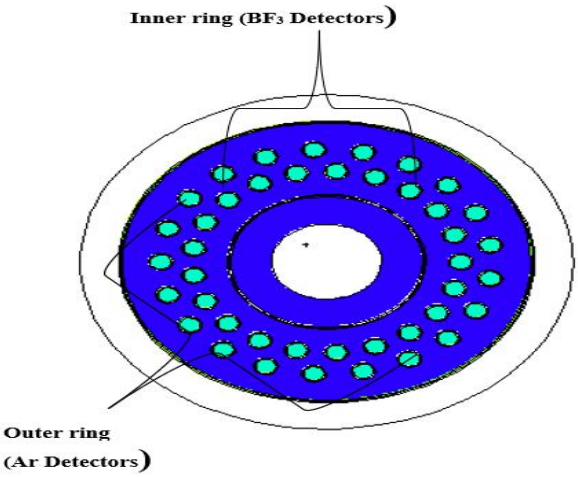
Inner ring (BF₃ Detectors)
Outer ring
(Ar Detectors)

(f)

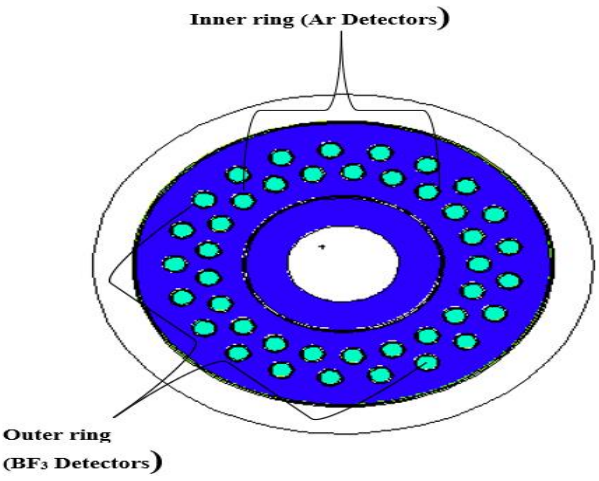
Inner ring (Ar Detectors)
Outer ring
(BF₃ Detectors)

(g)

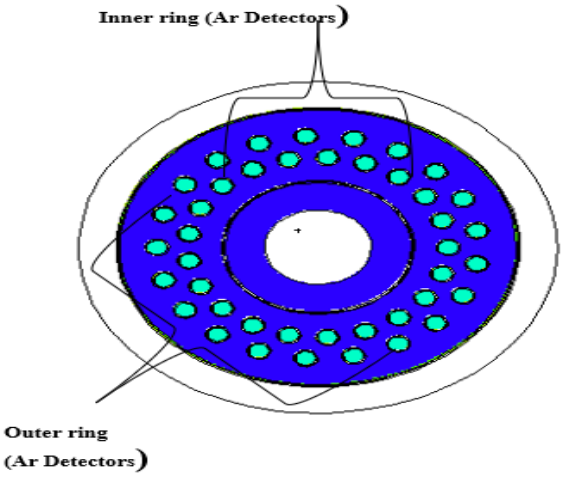

(h)

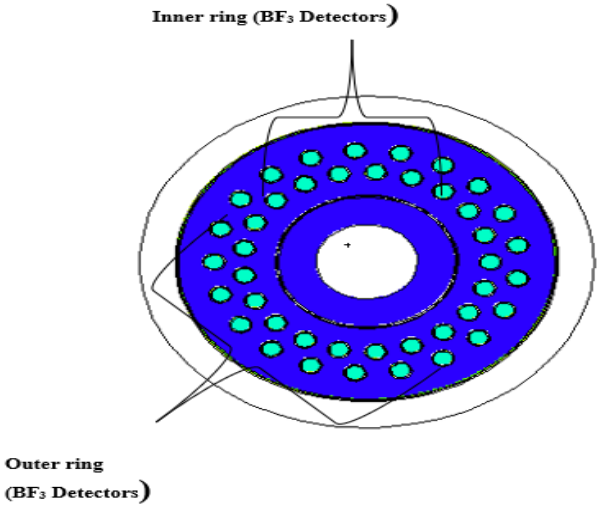

(i)

Fig. (1): Neutron detectors systems with different arrangements

3. RESULTS AND DISCUSSION

The effectiveness of the suggested systems and the pulse height distribution in various scenarios were assessed. Subsequently, a comparison was made between the output spectra obtained from them and the AWCC.

Fig. (2) illustrates the neutron energy distribution from 0- 0.25 eV for all the proposed designs. Figs. (3,4) we started to focus on specific regions at which we noticed slightly variation of energy deposition. Fig. (3) covers the range (0-0.005) eV and Fig. (4) covers the range (0.005-0.25) eV. We found that the design in which BF_3 outer ring and Ar inner ring gave the highest values in fig. (3) while in fig. (4) the highest value was to AWCC.

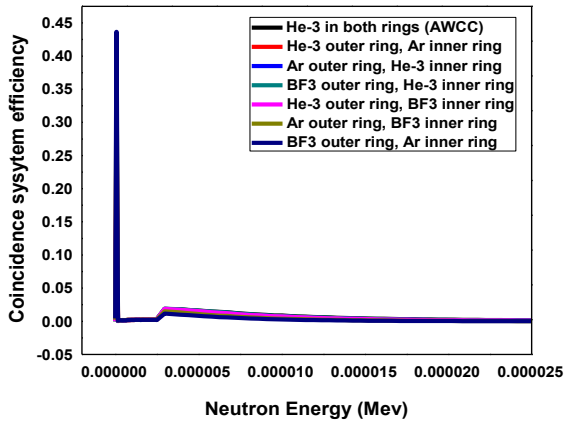

Fig. (2): Pulse height distribution for all the simulated coincidence neutron systems

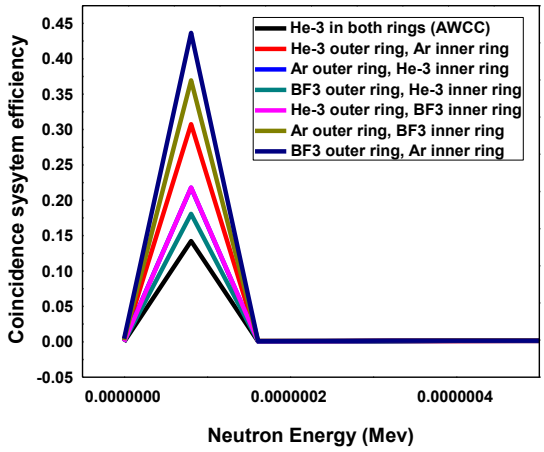

Fig. (3): Obtained spectrum from energy range (0-0.0005) keV

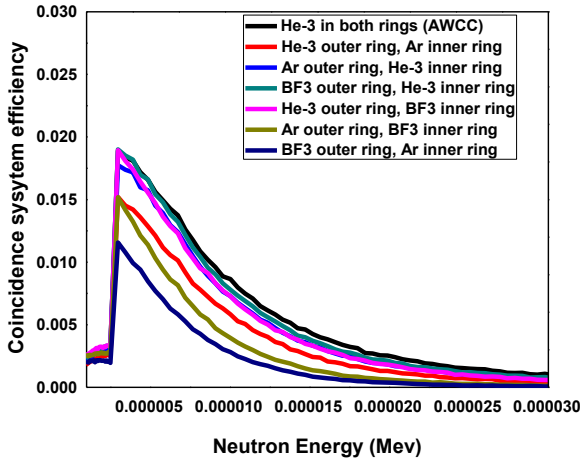

Fig. (4): obtained spectrum from energy range (0.0005-0.3) keV

With changing the neutron source type, we noticed some fluctuations in the range from 0-0.075 eV. Fig. (5) accumulates all the designs compared to AWCC using AmLi source. The spectrum (a) in fig. (5) illustrates the comparison between the outputs of AWCC and model (b) in fig. (1) which consists of He detectors in the outer ring of the design and Ar- detectors in the inner ring of the design. The comparison between the AWCC outputs and model (c) in fig. (1), where ^{3}He detectors are in the outer ring of the design and BF_3- detectors are in the inner ring, is shown in spectrum (b) in fig. (5). The comparison between the AWCC outputs and model (d) in fig. (1), where Ar- detectors are in the outer ring of the design and ^{3}He- detectors are in the inner ring, is shown in spectrum (c) in fig. (5). The contrast between the AWCC outputs and model € in fig. (1), where BF_3- detectors are in the outer ring of the design and ^{3}He- detectors are in the inner ring, is shown in spectrum (d) in fig. (5). Figure (5)'s spectrum € compares the outputs of the AWCC with model (f) in Figure (1), where BF_3- detectors are located in the inner ring of the design and Ar- detectors are in the outer ring. Figure (5)'s spectrum (f) compares the outputs of AWCC with the model (g) in Figure (1), wherein Ar- and BF_3- detectors are located in the inner and outer rings of the design, respectively. Figure (5)'s spectrum (g) compares the AWCC outputs to model (h) in Figure (1), where Ar- detectors are located in both design rings. Figure (5)'s spectrum (h) illustrates how the outputs are compared between the AWCC and model (i) in fig. (1), where BF_3-detectors are located in both design rings. We noticed that AWCC gave the lowest value at the range from 0-0.015 eV and after this range, the values mostly become higher or the same. The same behavior occurs using AmBe source and ^{252}Cf source as in figs. (6,7).

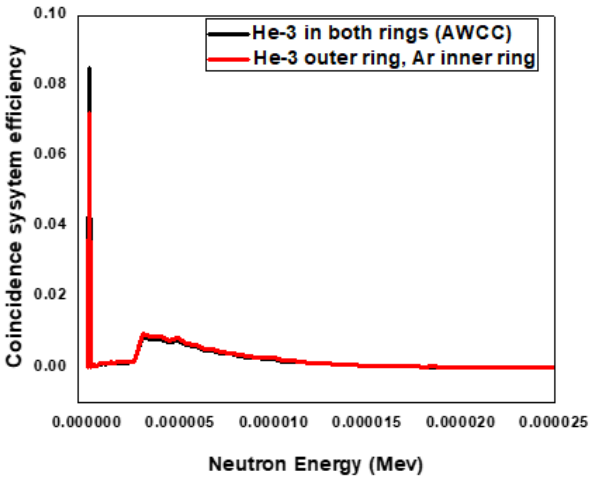

(a)

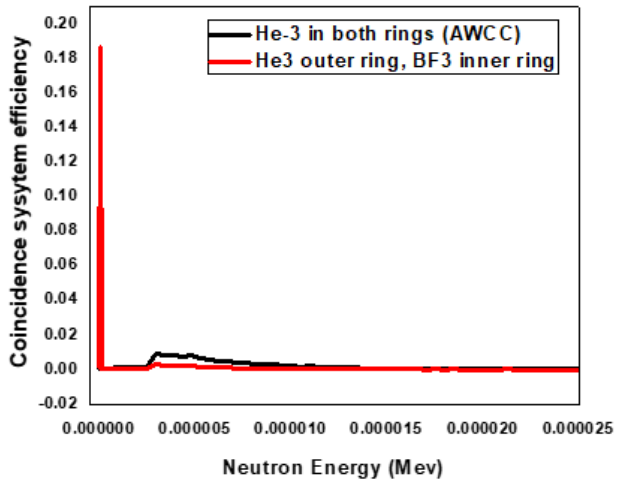

(b)

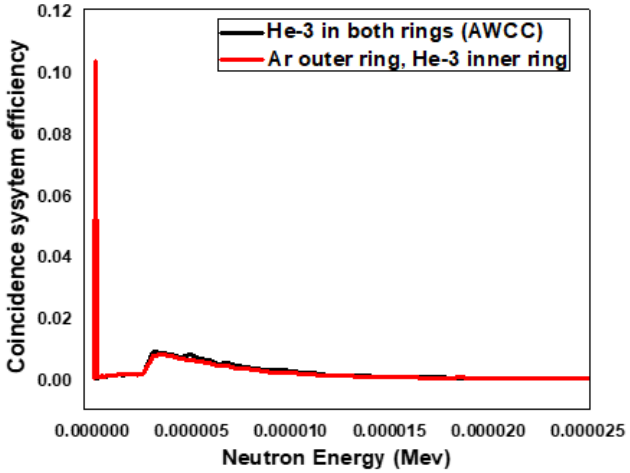

(c)

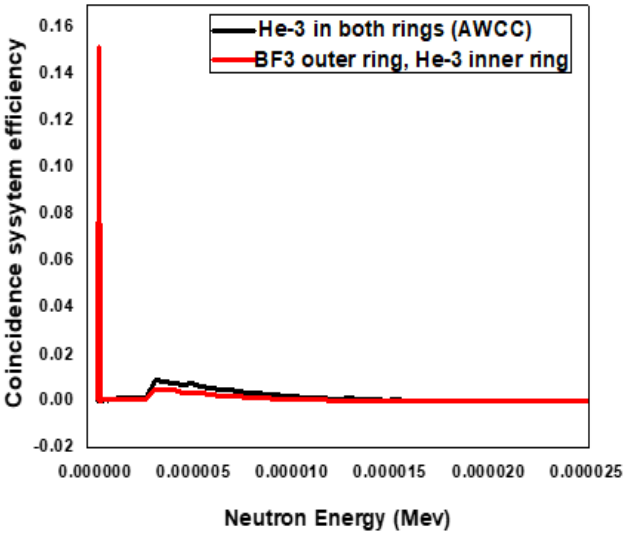

(d)

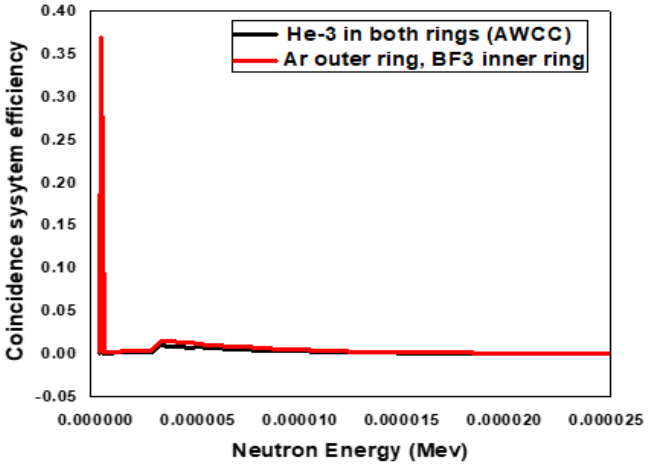

(e)

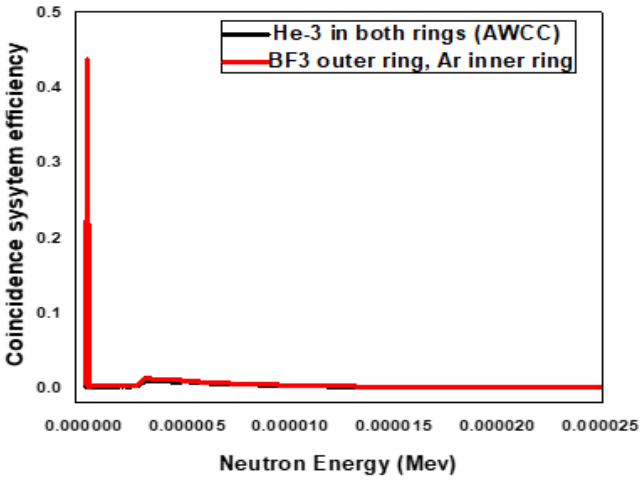

(f)

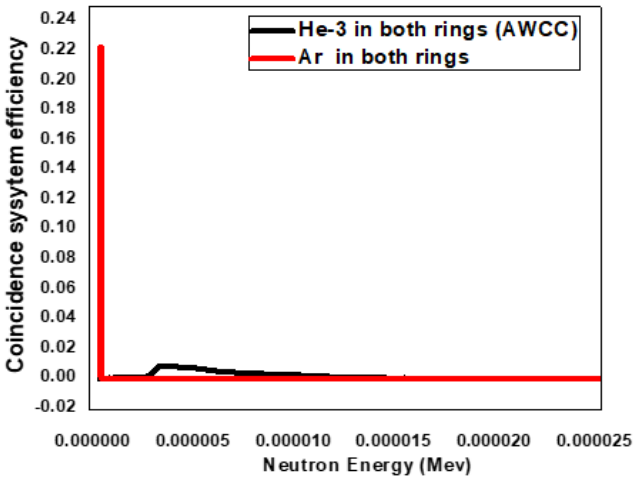

(g)

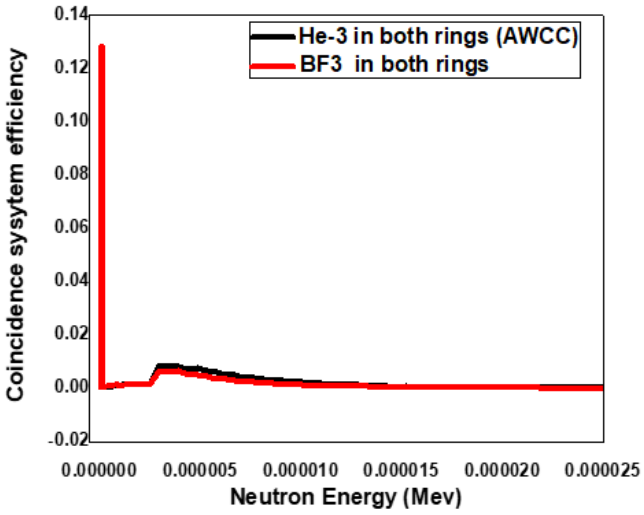

(h)

Fig. (5) Neutron distribution using AmLi source

In Fig.(6), we changed the neutron source to AmBe source and studied the effect of different neutron detector designs and arrangements in each model with the AWCC output. We found that AWCC gave the lowest value at the range from 0-0.015 eV in all the spectra and slight shifts in some spectra (g,h) and after this range the AWCC gives the same value of the system efficiency or higher than the others.

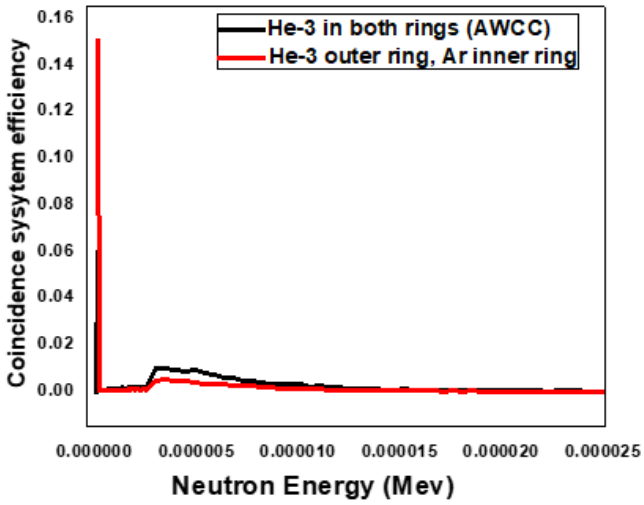

(a)

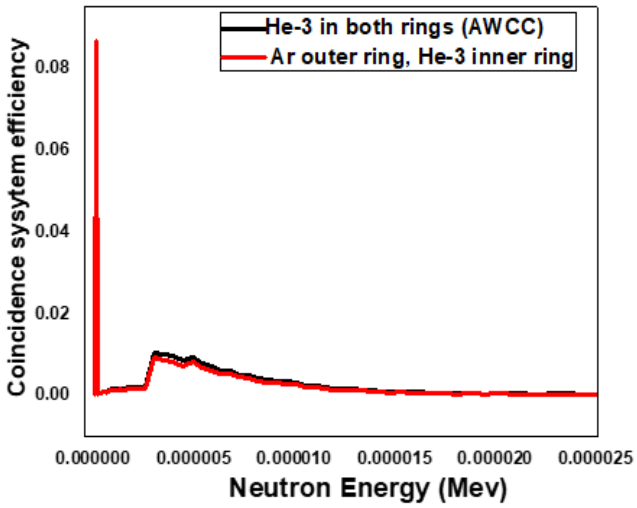
He-3 in both rings (AWCC)
Ar outer ring, He-3 inner ring
Coincidence sysytem efficiency
0.08
0.06
0.04
0.02
0.00
0.000000 0.000005 0.000010 0.000015 0.000020 0.000025
Neutron Energy (Mev)

(b)

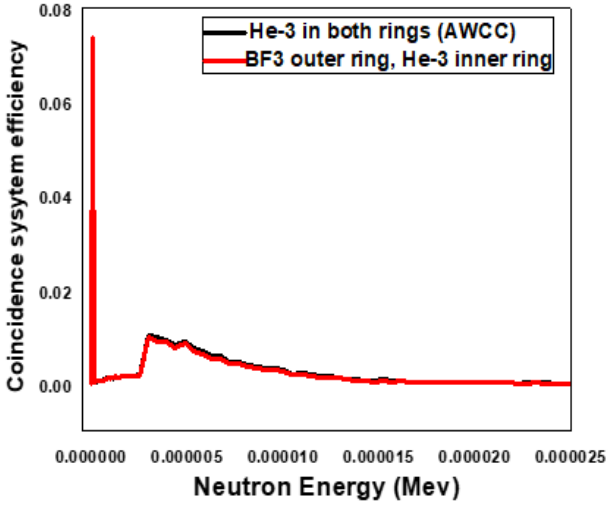
He-3 in both rings (AWCC)
BF3 outer ring, He-3 inner ring
Coincidence sysytem efficiency
0.08
0.06
0.04
0.02
0.00
0.000000 0.000005 0.000010 0.000015 0.000020 0.000025
Neutron Energy (Mev)

(e)

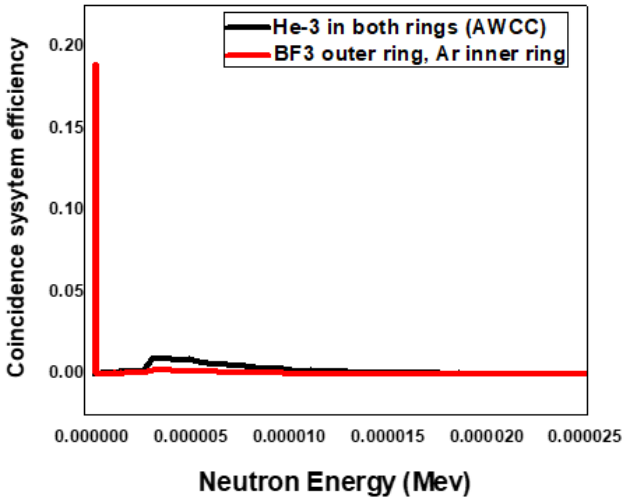
He-3 in both rings (AWCC)
BF3 outer ring, Ar inner ring
Coincidence sysytem efficiency
0.20
0.15
0.10
0.05
0.00
0.000000 0.000005 0.000010 0.000015 0.000020 0.000025
Neutron Energy (Mev)

(c)

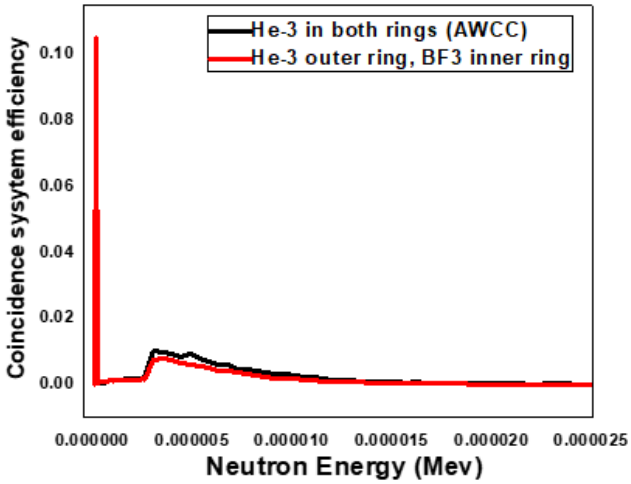
He-3 in both rings (AWCC)
He-3 outer ring, BF3 inner ring
Coincidence sysytem efficiency
0.10
0.08
0.06
0.04
0.02
0.00
0.000000 0.000005 0.000010 0.000015 0.000020 0.000025
Neutron Energy (Mev)

(f)

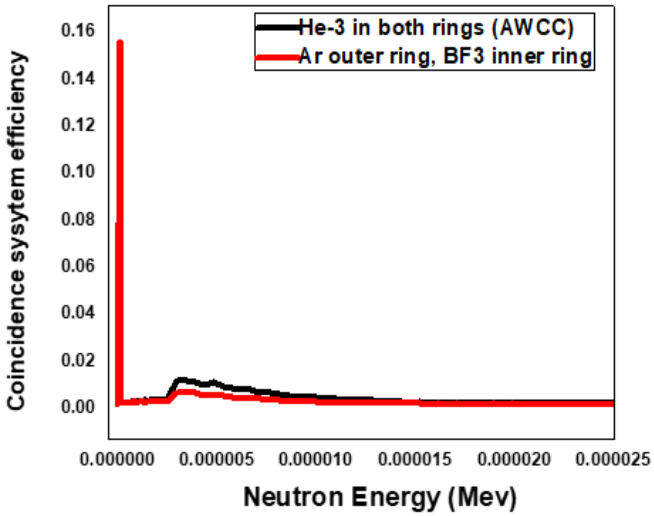
He-3 in both rings (AWCC)
Ar outer ring, BF3 inner ring
Coincidence sysytem efficiency
0.16
0.14
0.12
0.10
0.08
0.06
0.04
0.02
0.00
0.000000 0.000005 0.000010 0.000015 0.000020 0.000025
Neutron Energy (Mev)

(d)

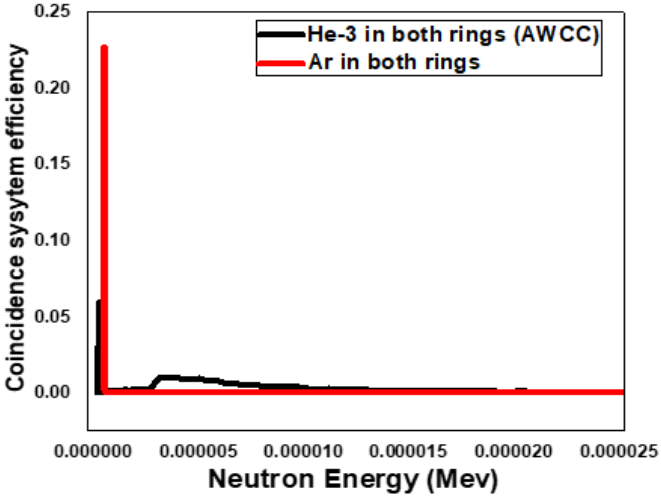
He-3 in both rings (AWCC)
Ar in both rings
Coincidence sysytem efficiency
0.25
0.20
0.15
0.10
0.05
0.00
0.000000 0.000005 0.000010 0.000015 0.000020 0.000025
Neutron Energy (Mev)

(g)

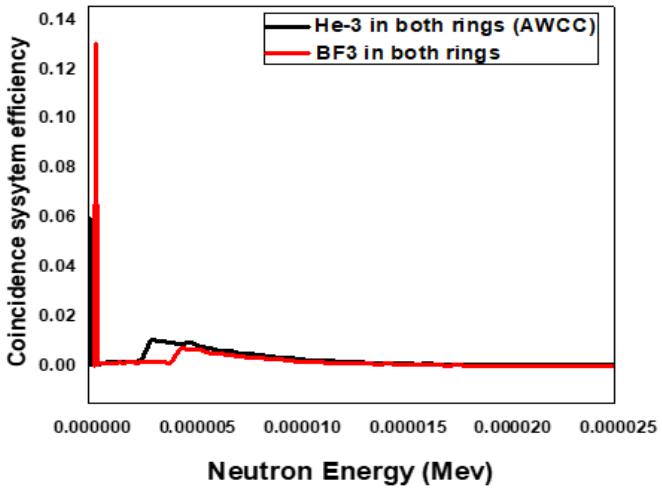

(h)

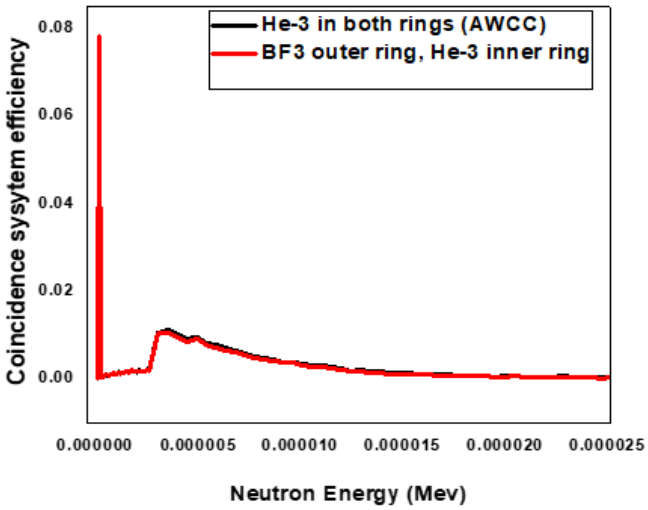

(c)

Fig. (6): Neutron distribution using AmBe source

By changing the neutron source to ^{252}Cf source in each design of neutron detectors as shown in fig.(7), we got the same behavior in the efficiency as in Figs. 5 and 6.

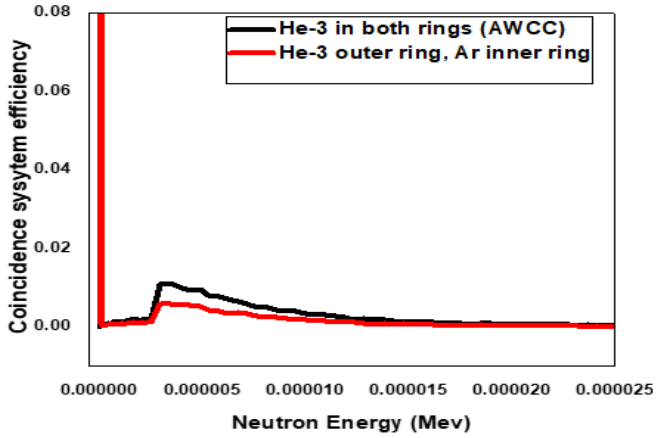

(a)

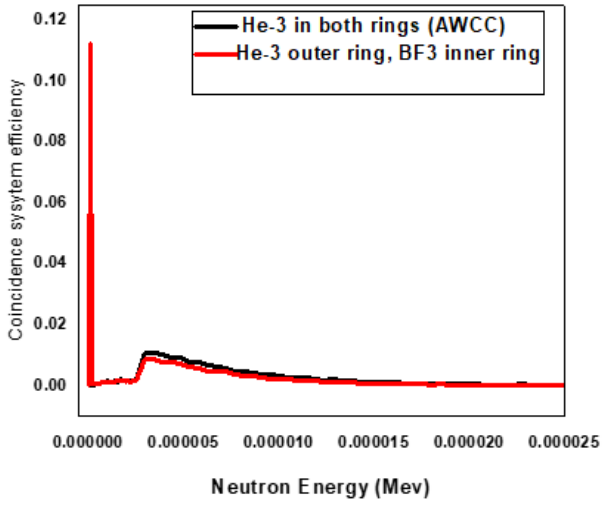

(d)

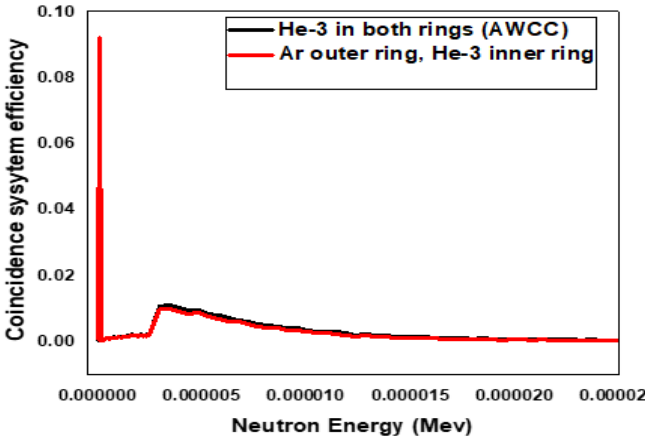

(b)

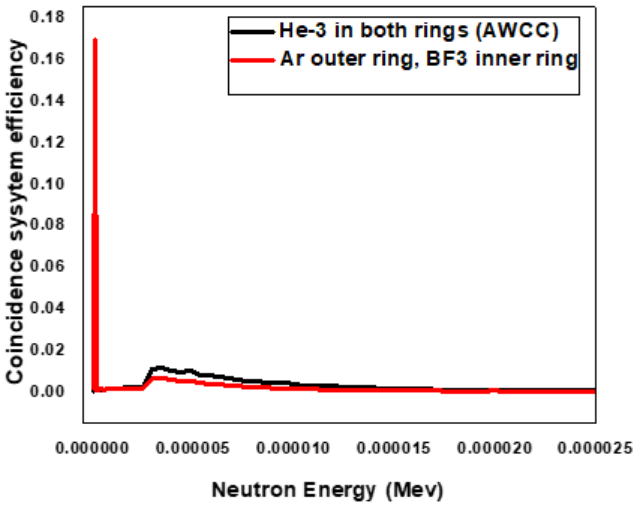

(e)

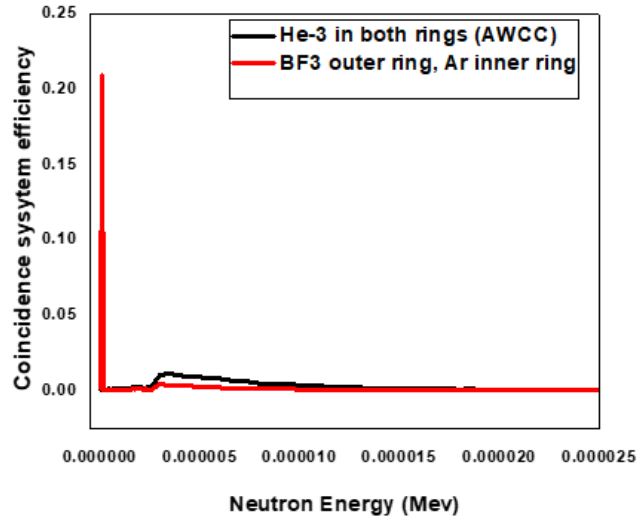

(f)

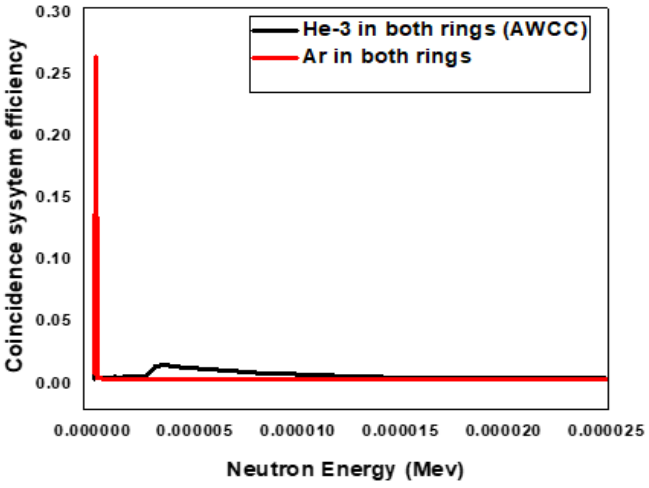

(g)

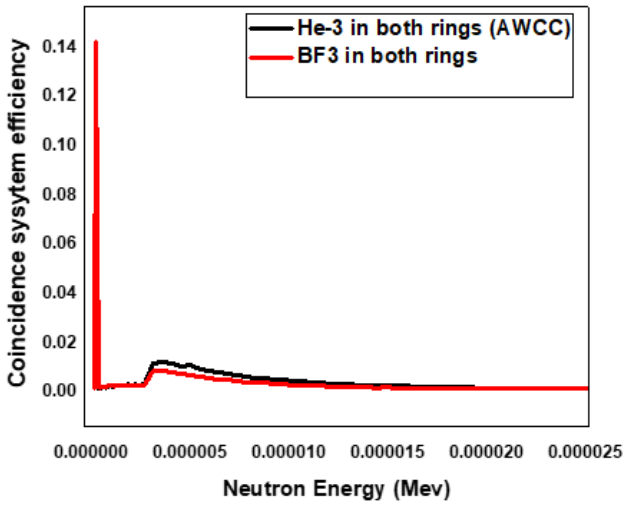

(h)

Fig. (7): Neutron distribution using ^{252}Cf source

5. CONCLUSION

To generate the liberated particles that are used as indicators in the nuclear material testing, these models simulate coincidence neutron systems. The models were evaluated by comparing their coincidence efficiency systems to the active-well neutron coincidence counter (AWCC) using typical safeguards detectors and the simulation of nuclear data for SNM. The three different neutron sources were used (AmLi, AmBe and ^{252}Cf) The comparison was carried out between the standard model of AWCC and the proposed systems in the energy range which covered the thermal neutron region (0-0.025) KeV. No single model performed noticeably better than the others and we could recommend using any of the proposed designs to replace AWCC. However, each difference's impacts have been described and should be taken into consideration while selecting a model.

ACKNOWLEDGMENTS

The authors are grateful to The Egyptian Atomic Energy Authority for their support and for providing an appropriate environment for continuity in the research field.

REFERENCES

[1] P. Peerani, G. Bosler, I. Cherradi and P. Schwalbach. "Computational Calibration of Neutron Collars for the Verification of HEU Fuel Elements", Proceeding of the 45th INMM Annual Meeting, Orlando (FL), 18-22 July 2004.

[2] H. Tagziria, P. Peerani, W. Koehne and P. Schwalbach, "On-line verification of MOX Fuel Magazines Using Monte Carlo Simulation", Esarda symposium, London May 2005.

[3] P. Peerani, H Tagziria and M. Looman, "Real time simulation of neutron counters, Radiation Measurements 43 (2008) 1506-1510

[4] H. Tagziria, P. Peerani, P. de Baere and P. Schwalbach H. "Monte Carlo Modelling of a Neutron Coincidence Counter for the Verification of PuO_2 cans", Nuc. Ins. & Meth. A580 (2007) 377-379

[5] Marc Looman, Paolo Peerani, Hamid Tagziria, Monte Carlo simulation of neutron counters for safeguards applications, Detectors and Associated Equipment, Volume 598, Issue 2, 11 January 2009, Pages 542-550

[6] Jay P. Joshi, Timothy J. Aucott, Mustafa Siddiqi, William S. Charlton, Calibration of Active Well

Coincidence Counter (AWCC) With Highly Enriched Uranium (heu) And Ambe Active Neutron Interrogation Source at The Savannah River National Laboratory, INMM, 2020.

[7] H. Tagziria, M. Looman, The ideal neutron energy spectrum of ^{241}AmLi $(\alpha,n)^{10}$B sources, Applied Radiation and Isotopes, Volume 70, Issue 10, October 2012, Pages 2395-2402

[8] H.O. Menlove, C.D. Rael, the optimization and calibration of the AWCC using ^{252}Cf interrogation and the comparison with an AmLi neutron source, Los Alamos National Laboratory Report LA-UR-15-29620, 2015.

[9] H.O. Menlove, S.H. Menlove, C.D. Rael, the development of a new, neutron, time correlated, interrogation method for measurement of U-235 content in LWR fuel assemblies, Nucl. Instrum. Methods Phys. Res. A 701 (2013) 72–79.

[10] Azaree Lintereur, Kenneth Conlin, James Ely, Luke Erikson, Richard Kouzes, Edward Siciliano, David Stromswold, Mitchell Woodring, ^{3}He and BF_3 neutron detector pressure effect and model comparison, Nuclear Instruments and Methods in Physics Research A 652 (2011) 347–350.

[11] Syed Naeem Ahmed, Physics and Engineering of Radiation Detection, second edition, Elsevier, ISBN:978-0-12-801363-2, (2015) 201-202.

[12] F. Casagrandei, P. Cennini and Xuan Li, The Argon Gas Detectors for the Fission Measurement in the First Energy Amplifier Test (FEAT), EUROPEAN ORGANIZATION FOR NUCLEAR RESEARCH, CERN-AT-95-05.

[13] E. Diana, K. Kanaki, R.J. Hall-Wiltonb, P. Zagyvaia, Sz. Czifrus, Neutron activation and prompt gamma intensity in Ar/CO2-filled neutron detectors at the European Spallation Source, Applied Radiation and Isotopes, Volume 128, October 2017, Pages 275-286.

[14] R.K. Weinmann-Smith, M.T. Swinhoe, A. Trahan, M.T. Andrews, H.O. Menlove, A. Enqvist, A comparison of Monte Carlo fission models for safeguards neutron coincidence counters, Nuclear Inst. and Methods in Physics Research, A 903 (2018) 99–108.

[15] MCNP - A General Monte Carlo N-Particle Transport Code, Version 5, Volume I: Overview and Theory" (LA-UR-03-1987).

[16] MCNP - A General Monte Carlo N-Particle Transport Code, Version 5, Volume II: User's Guide" (LA-CP-03-0245).

[17] MCNP - A General Monte Carlo N-Particle Transport Code, Version 5, Volume III: Developer's Guide" (LA-CP-03-0284).

[18] John S. Hendricks Martyn T. Swinhoe Andrea Favalli, Monte Carlo N-Particle Simulations for Nuclear Detection and Safeguards, https://doi.org/10.1007/978-3-031-04129-7.

[19] H.O. Menlove, Description and operation manual for the active well coincidence counter, LA-7823-M, Los Alamos, 1979.

[20] W. El-Gammala, W.I. Zidana, E. Elhakimb, A proposed semi-empirical method for ^{235}U mass calibration of the active-well neutron coincidence counter, Nuclear Instruments and Methods in Physics Research A 565 (2006) 731–741.